

VFM-UDA++: Improving Network Architectures and Data Strategies for Unsupervised Domain Adaptive Semantic Segmentation

Brunó B. Englert Gijs Dubbelman
Eindhoven University of Technology
{b.b.englert, g.dubbelman}@tue.nl

Abstract

Unsupervised Domain Adaptation (UDA) has shown remarkably strong generalization from a labeled source domain to an unlabeled target domain while requiring relatively little data. At the same time, large-scale pretraining without labels of so-called Vision Foundation Models (VFMs), has also significantly improved downstream generalization. This motivates us to research how UDA can best utilize the benefits of VFMs. The earlier work of VFM-UDA showed that beyond state-of-the-art (SotA) results can be obtained by replacing non-VFM with VFM encoders in SotA UDA methods. In this work, we take it one step further and improve on the UDA architecture and data strategy themselves. We observe that VFM-UDA, the current SotA UDA method, does not use multi-scale inductive biases or feature distillation losses, while it is known that these can improve generalization. We address both limitations in VFM-UDA++ and obtain beyond SotA generalization on standard UDA benchmarks of up to +5.3 mIoU. Inspired by work on VFM fine-tuning, such as Rein, we also explore the benefits of adding more easy-to-generate synthetic source data with easy-to-obtain unlabeled target data and realize a +6.6 mIoU over the current SotA. The improvements of VFM-UDA++ are most significant for smaller models, however, we show that for larger models, the obtained generalization is only 2.8 mIoU from that of fully-supervised learning with all target labels. Based on these strong results, we provide essential insights to help researchers and practitioners advance UDA.

1. Introduction

Developing models that adapt to diverse data distributions, including previously unseen distributions, is a key challenge in computer vision. This challenge becomes particularly pronounced when models encounter significant data distribution shifts between the training and testing conditions. In dense prediction tasks like semantic segmentation, obtain-

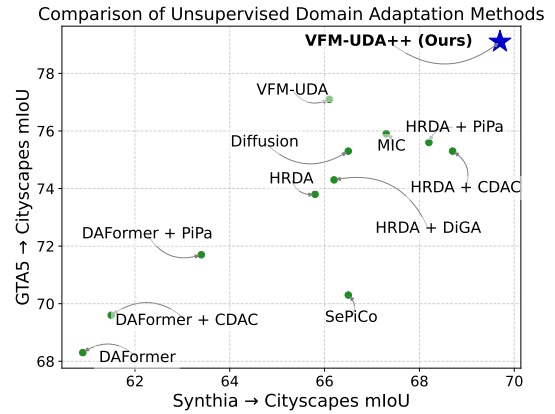


Figure 1. **VFM-UDA++ compared to previous state-of-the-art methods.** Result of VFM-UDA++ is shown in blue for the popular benchmarks GTAV to Cityscapes and SYNTHIA to Cityscapes.

ing accurate pixel-level labeled data is labor-intensive, inherently limiting data scale and diversity. This limitation can hinder adaptation to real-world variability.

Unsupervised Domain Adaptation (UDA) [17] aims to bridge a shift in data distribution, often called *domain gap*, by adapting a model trained on a labeled *source domain* to perform well in an unlabeled *target domain*. Without adaptation, the domain gap between source and target caused by variations in location, weather, lighting, textures, sensor properties, class distributions, etc., can lead to overfitting on the source domain and poor generalization to the target domain. UDA techniques have benefited from increasingly powerful vision models, progressing from CNNs pretrained on ImageNet1K [18], multi-scale Vision Transformers (ViTs) [18], to Vision Foundation Models (VFMs) [12]. These VFMs [13, 14, 30], are pretrained on extensive datasets with weak- and/or self-supervision and exhibit impressive downstream generalization [30]. Initial research combining VFMs with UDA was conducted in [12], obtaining SotA results but also revealing that not all UDA techniques remain equally effective when applied

with VFM encoders and that not all VFM encoders perform equally well in UDA for semantic segmentation.

We continue on the line of VFM-UDA [12] and observe that UDA methods using traditional non-VFM multi-scale architectures, like in MIC [20], pretrained on ImageNet [20], obtain remarkably strong results. However, they underperform using single-scale ViT [11] models pretrained on the same ImageNet dataset [12]. In contrast, single-scale ViTs pretrained with advanced self-supervised methods, like DINOv2 [30], have demonstrated superior performance in UDA tasks [12]. This raises fundamental questions about the influence of the architecture and its pretraining on UDA and whether its generalization can be improved further by combining a multi-scale architecture with strong VFM pretraining. Another development based on the strong downstream generalization of VFMs, is low-rank fine-tuning. Methods such as Rein [47] have shown that generalization to a target can significantly increase by adding more (synthetic) source data without using any target data. When using the same source data, such source-only fine-tuning of VFMs is not better than UDA, which can also use target data. However, fine-tuning performance is on par with UDA simply by using more source data. Because UDA could also utilize easy-to-generate synthetic source data and especially easy-to-obtain unlabeled real data, it is natural to research if and how UDA generalization can scale by using more data. Considering the above, this work addresses the following research questions: (i) How can VFM-UDA be improved further with architectural advancements? (ii) How can VFM-UDA generalization be improved by scaling data? (iii) To what extent do these improvements reduce the generalization gap between UDA and fully-supervised learning?

Regarding our first research question, we examine the current SotA method, VFM-UDA, observing that, unlike non-VFM UDA methods, it does not utilize multi-scale inductive biases or feature distance losses. Such techniques are used by earlier non-VFM UDA methods that currently do not provide SotA generalization anymore. Still, it is meaningful to research whether their underlying fundamental principles can be reused or replaced with modern techniques to advance VFM-UDA. We observe that straightforwardly using multi-scale VFMs and previously used feature distance losses does not lead to optimal UDA generalization and can even reduce it. Therefore, we explore and provide alternatives that do improve generalization and assess them on multiple standard UDA benchmarks. This results in beyond SotA generalization, as can be viewed in Fig. 1.

Regarding our second and third research questions, we test with various source and target data extensions to better understand the underlying data principles. Scaling data in UDA is natural as one of its original use cases was to train models on easy-to-generate synthetic source data and

easy-to-obtain unlabeled target data. The most important learning is that by scaling data, UDA generalization gets very close, *i.e.* **only 2.8 mIoU difference**, to a strong fully-supervised VFM baseline. This result is extraordinarily close, and our experiments assess whether further advancing UDA is realistic. We observe that subtle label-definition ambiguities between the source and target and labeling errors start to limit UDA. From this, we derive novel insights and recommendations on efficiently and effectively advancing UDA in future research.

Our contributions are as follows:

- **Advancements in UDA:** We evaluate the integration of ViT-based VFMs with modern multi-scale inductive biases and feature distillation losses, showing improved generalization on multiple standard UDA benchmarks.
- **Scaling UDA with data:** We improve UDA generalization further by exploiting its key property of being able to use easy-to-generate synthetic data and easy-to-obtain unlabeled data, investigating how greater data diversity influences UDA.
- **Novel UDA insights:** Our enhancements have brought UDA very close to a realistic upper-bound generalization and, from this, we derive insights that can guide future research towards practical application of UDA.

2. Related Work

Our contributions build on a significant body of previous UDA work [3, 4, 12, 18–20, 31, 39, 45, 46, 53]. Over years of research, *pseudo-labeling* [2, 19, 20, 24, 43, 49] emerged as the core (self-supervised) UDA technique, using target domain predictions as pseudo-labels to guide adaptation, often stabilized through Exponential Moving Average (EMA) models. Effective *learning rate optimization* strategies, such as using different rates for encoder and decoder layers and employing learning rate warm-up phases [18], have proven critical for preserving robust pretrained features while fine-tuning for downstream tasks. *Data augmentation* and source-target sample mixing [42] expose models to diverse spatial and semantic contexts, promoting robustness to pixel-space differences. *Architectural enhancements*, including multi-scale encoders and attention modules [18, 19], are designed to capture better fine details and contextual information necessary for accurate dense predictions. To tackle *class imbalance*, methods like Rare Class Sampling [18] mitigate issues in poorly balanced datasets, reducing the risk of class prediction collapse. *Feature distance loss* [18] aligns source and/or target feature distributions by minimizing discrepancies between their feature representations. Finally, *masked image consistency* [18] techniques enhance contextual reasoning by enforcing consistent predictions across masked and unmasked views.

A modern and complementary (non-UDA) technique

to improve model generalization is using Vision Foundation Model (VFM) pre-training. VFMs have significantly advanced computer vision by leveraging large-scale, diverse data for versatile downstream applications. For instance, CLIP [33] uses contrastive learning [5] on image-text pairs for robust visual representations, while MAE [16] reconstructs pixel-level data through masked image modeling [51]. DINOv2 [30], a recent self-supervised method, achieves strong cross-domain generalization without labeled data. However, most VFMs rely on single-scale ViT [11] architectures, which can be less suitable for dense tasks like semantic segmentation. Recent efforts, such as the ViT-Adapter [6], address this by enabling multi-resolution feature output. Initial research combining VFMs with UDA was conducted in [12] but did not include contemporary multi-resolution methods such as the ViT-Adapter.

To our knowledge, combining VFMs with multi-scale architectures and more diverse datasets for UDA has not been fully explored. This work addresses this gap, providing a strong foundation for advancing UDA methods for future research and assessing their real-world applicability.

3. Methodology

Here, we present the details of the **VFM-UDA++** method, of which ablations support its design choices in Sec. 4. For its components, we start with VFM-UDA, extend it with multi-scale inductive biases in its encoder and decoder, and improve its UDA learning strategy with feature distances losses. We clarify that the components we introduce on top of the original VFM-UDA are new to UDA but not fundamentally novel techniques. Still, introducing these components in VFM-UDA in a way that they contribute to its generalization, is not trivial, as demonstrated in our ablations. Experiments in Sec. 4 demonstrate beyond SotA generalization of VFM-UDA++ on multiple standard and non-standard benchmarks. These results show levels of generalization that are close to fully-supervised learning, and from this, novel findings and insights can be obtained.

3.1. VFM-UDA++

The VFM-UDA++ architecture, shown in Fig. 2, combines a ViT-based encoder pretrained with DINOv2, extended with a ViT-Adapter to output multi-scale feature maps, and paired with our custom BasicPyramid decoder. VFM-UDA++’s training strategy builds on top of VFM-UDA [12], extending it with AM-Radius loss [34].

Core UDA technique: The core component of the VFM-UDA++ method is pseudo-labeling, an essential and thus common approach in practically all SOTA UDA methods [2, 19, 20, 24, 43, 49]. In naive pseudo-labeling, the

model generates predictions for the unlabeled target domain, treating these predictions as labels for subsequent training iterations. While this approach provides a self-supervised signal to learn domain-specific features, it is highly susceptible to noise and error accumulation. As a result, training on pseudo-labels can reinforce incorrect predictions, causing the model to drift away from the desired target distribution. To address these issues, VFM-UDA++ employs strategies similar to those used in MIC [20], such as Exponential Moving Average (EMA) [41] teacher model, which stabilizes pseudo-label generation by maintaining a smoothed teacher model through iterative weight updates. Pseudo-label weighting [15, 29] is also used to emphasize high-confidence predictions and diminish the influence of noisy, uncertain labels, further enhancing stability and alignment between source and target domains. This is particularly important in the early stages of training when pseudo labels are still incorrect.

Multi-scale VFM encoder: Vision Transformers (ViTs) typically output single-scale features, which can be limiting for tasks like segmentation that benefit from multi-scale, high-resolution features. To address this, and unlike VFM-UDA [12], we extend ViT-based VFMs [30] with a ViT-Adapter [6] that outputs multi-resolution features, enabling accurate segmentation for object edges and small objects. Our experiments primarily utilize DINOv2 as the ViT-based VFM due to its robust performance, as shown in the supplementary material.

Multi-scale decoder: To use the benefits of the multi-resolution features generated by the ViT-Adapter, we pair it with our custom BasicPyramid decoder. This decoder uses only convolutions [25], ReLU [1], and Batch-Norm [22], and it progressively scales up features while aggressively reducing channel size at higher resolutions, see Fig. 2. This design choice enables faster inference at high resolution, differentiating it from DAFormer [18], which doesn’t use a pyramid structure and instead scales all features to a single high-resolution feature. As detailed in Sec. 4.6, our BasicPyramid decoder achieves the best balance of computational efficiency and segmentation accuracy when compared to alternatives, including DAFormer [18], HRDA [19], and Mask2Former [7], making it the preferred decoder for VFM-UDA++.

Auxiliary training techniques: To optimize UDA performance, we explore a range of training strategies, and each is re-evaluated in the context of multi-scale ViT-based VFMs to see their impact on domain alignment and generalization. Our final configuration takes advantage of techniques such as learning rate multiplier between encoder and decoder

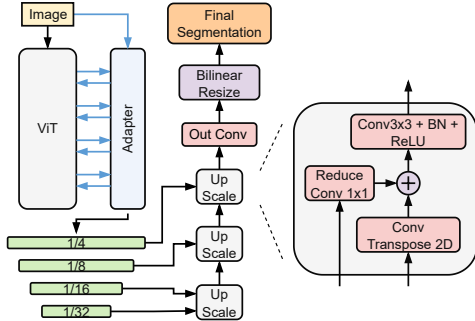


Figure 2. **VFM-UDA++ multi-scale architecture.** VFM-UDA++ adds multi-scale inductive bias to VFM-UDA by equipping it with a ViT-Adapter [6] and a custom image pyramid decoder *BasicPyramid*.

layers, Domain Adaptation via Cross-domain Mixed Sampling (DACS) [42], Rare Class Sampling [18] to improve the representation of uncommon categories and Masked Image Consistency (MIC) [20] for robust spatial consistency.

Additionally, we compare our proposed feature alignment loss with DAFormer’s Feature Distance Loss [18]. Unlike DAFormer, which relies on explicit masking of stuff and thing classes, VFM-UDA++ leverages VFM feature extractors trained on large-scale, diverse datasets, allowing them to inherently capture both stuff and thing class types in their feature representations. As a result, our method eliminates the need for stuff-thing masking, enabling the feature extractor to be applied to both the source and target domains, which was not the case for DAFormer’s Feature Distance loss. Furthermore, we introduce a projector head to enable flexibility in feature alignment. This component decouples feature extraction from the student model, allowing for the use of a more expressive and larger teacher model.

3.2. Implementation details

The VFM-UDA++ architecture is a ViT encoder pretrained with DINOv2 coupled with ViT-Adapter [6] and the BasicPyramid decoder. Training uses the AdamW [27] optimizer, with a linear warm-up learning rate for the first 1,500 iterations, followed by linear decay. The decoder learning rate was set at 1.4×10^{-4} , while the encoder used a learning rate of 1.4×10^{-5} and the DINOv2 pretrained ViT’s layers have 0.9 layerwise decay. In all experiments, no matter the dataset, the training iterations is 40,000 with a batch size of 8. For pseudo-label generation, we use horizontal flip aggregation to minimize pseudo-label noise and the threshold for accepted pseudo-labels is 0.968 [18, 20]. We use image masking with a 0.7 drop rate, the same as in MIC [20].

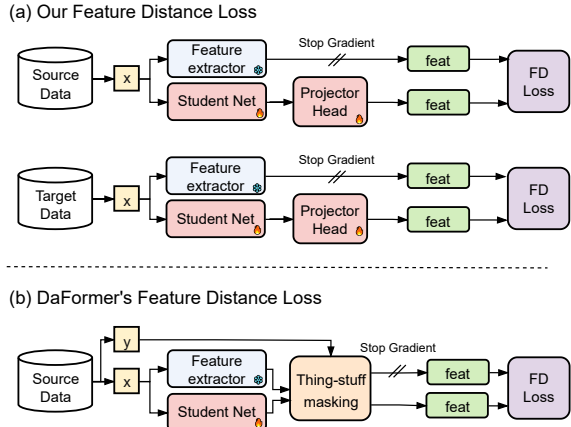


Figure 3. **Our proposed feature distance loss compared to that of DAFormer.** Our VFM Feature distance loss works on both source and target data. This is different from the DAFormer [18] feature distance loss, where labels are a crucial part of the FD loss and thus can only be used for the source data where labels are available.

4. Experiments and results

The experiments are designed to answer our research questions: (i) How can UDA be improved further with VFM architectural advancements? (ii) How can UDA generalization be improved by scaling data? (iii) How much do these improvements improve the generalization gap between UDA and fully-supervised learning? We start by demonstrating the beyond SotA results of the VFM-UDA++ approach over existing UDA approaches on multiple popular UDA benchmarks. We then continue showing the impact of using more data on non-VFM and VFM UDA methods for both in-target and out-of-target generalization, as in [32]. To highlight the significance of the methodological improvement contained in VFM-UDA++ and that of using more data, we compare it to several fully-supervised baselines trained with all target-domain labels. We then continue with ablations on the importance of data selection strategies and finish with ablations on the architectural advancements of VFM-UDA++.

4.1. Results on standard benchmarks

As can be observed from Tab. 1 for the GTAV to Cityscapes benchmark, VFM-UDA++ consistently outperforms previous methods. Especially for the smaller, efficient models, the gains of VFM-UDA++ are most pronounced, reaching up to +5.3 mIoU. Furthermore, using its architectural advancements, VFM-UDA++ consistently outperforms VFM-UDA at all model sizes. The relevance of VFM-UDA++ is most clearly demonstrated by observing that even its smallest model (76.6 mIoU @ 27M) outperforms the SotA non-VFM UDA method MIC (75.9 mIoU @ 86M), despite having more than $3 \times$ fewer parameters. The same trend is

Method	#Parameters	Backbone	mIoU CS
CorDA [46] \w depth	48M	ResNet-101	56.6
ProDA [53]	48M	ResNet-101	57.5
SePiCo [49]	86M	MiT-5	70.3
DAFormer [18]	86M	MiT-5	68.3
DAFormer [18] + CDAC [45]	86M	MiT-5	69.6
DAFormer [18] + PiPa [3]	86M	MiT-5	71.7
HRDA [19]	86M	MiT-5	73.8
HRDA [19] + DiGA [39]	86M	MiT-5	74.3
HRDA [19] + CDAC [45]	86M	MiT-5	75.3
Diffusion [31]	86M	MiT-5	75.3
HRDA [19] + PiPa [3]	86M	MiT-5	75.6
MIC [20]	86M	MiT-5	75.9
DCF [4] \w depth	86M	MiT-5	77.7
VFM-UDA [12]	27M	DINOv2-S	71.3
VFM-UDA [12]	88M	DINOv2-B	77.1
VFM-UDA [12]	334M	DINOv2-L	78.4
Source-only	334M	DINOv2-L	71.8
VFM-UDA++	27M	DINOv2-S	76.6 \uparrow +5.3
VFM-UDA++	88M	DINOv2-B	79.1 \uparrow +2.0
VFM-UDA++	334M	DINOv2-L	79.8 \uparrow +1.4
Oracle	334M	DINOv2-L	85.0

Table 1. **GTAV to Cityscapes benchmark.** VFM-UDA++ consistently outperforms previous methods. The provided deltas for VFM-UDA++ are to VFM-UDA for the same model size.

Method	Backbone	Source	Target	mIoU
ProDA [53]	ResNet-101	Synthia	Cityscapes	55.5
DAFormer [18]	MiT-5	Synthia	Cityscapes	60.9
DAFormer [18] + CDAC [45]	MiT-5	Synthia	Cityscapes	61.5
DAFormer [18] + PiPa [3]	MiT-5	Synthia	Cityscapes	63.4
HRDA [19]	MiT-5	Synthia	Cityscapes	65.8
VFM-UDA [12]	DINOv2-B	Synthia	Cityscapes	66.1
HRDA [19] + DiGA [39]	MiT-5	Synthia	Cityscapes	66.2
Diffusion [31]	MiT-5	Synthia	Cityscapes	66.5
SePiCo [49]	MiT-5	Synthia	Cityscapes	66.5
MIC [20]	MiT-5	Synthia	Cityscapes	67.3
HRDA [19] + PiPa [3]	MiT-5	Synthia	Cityscapes	68.2
HRDA [19] + CDAC [45]	MiT-5	Synthia	Cityscapes	68.7
VFM-UDA++	DINOv2-B	Synthia	Cityscapes	69.7 \uparrow +1.0
SePiCo [49]	MiT-5	Cityscapes	Darkzurich	45.4
MIC [20]	MiT-5	Cityscapes	Darkzurich	60.2
VFM-UDA [12]	DINOv2-B	Cityscapes	Darkzurich	67.4
VFM-UDA++	DINOv2-B	Cityscapes	Darkzurich	68.7 \uparrow +1.3

Table 2. **Other popular UDA benchmarks.** VFM-UDA++ consistently outperforms prior methods across all benchmarks including challenging settings like Cityscapes-to-Darkzurich and Synthia-to-Cityscapes.

observed when comparing VFM-UDA++ on other standard UDA benchmarks in Tab. 2 including one real-to-real scenario. Also here, VFM-UDA++ outperforms all other UDA methods with gains of +1.3 mIoU compared to its predecessor VFM-UDA.

4.2. Scaling data and UDA upper bound

The next step to improve VFM-UDA++ is utilizing UDA’s advantage of using easy-to-generate synthetic data and easy-to-obtain unlabeled read data. The datasets used for the combined labeled source dataset *All-synth* are GTA5 [35], SYNTHIA [36], and Synscapes [48], and have a total of 59,367 images. The datasets used for the combined unlabeled target dataset *All-real* are Cityscapes [8],

BDD100K [52], Mapillary Vistas [28], ACDC [38], and DarkZurich [9]. The *All-real* dataset has a total of 41,356 images that cover diverse weather, lighting, and environmental conditions. The ablations for selecting these datasets and their impact are provided in Sec. 4.5. We refer to the *All-synth* to *All-real* as the *All-in* benchmark and it has two goals. The first goal is precisely the same as in GTAV to Cityscapes, i.e., to perform well on the validation split of Cityscapes. We call this in-target generalization. The second goal is to perform well in out-of-target generalization, measured on the WildDash2 dataset. This is relevant for applications where the exact data distribution the model will encounter during deployment is unknown beforehand.

In Tab. 3 we report the results on the *All-in* benchmark and observe both the generalization of VFM-UDA and VFM-UDA++ scales well with data. However, the non-VFM UDA method MIC does not scale and drops when more data is added. In the data ablations of Sec. 4.5 we go deeper into what causes this drop and see that it is not unique to only non-VFM UDA. When comparing the result of the largest VFM-UDA++ model 82.2 mIoU with that of the oracle 85.0 mIoU, we obtain an unprecedentedly small gap of **only 2.8 mIoU** between UDA and a strong fully-supervised baseline. This is a key result of our work and its significance can be appreciated even more from the experiment in the next section.

4.3. Distance to supervised learning

In this experiment, we compare the strong generalization of VFM-UDA++ with more supervised baselines. We use a fully-supervised baseline with the same architecture, i.e. the oracle, but also other baselines with larger architectures. We also compare to synthetic source-only supervised learning such as Rein [47] and, more importantly, a version of source-only supervised learning where we use the entire *All-real* dataset except the target Cityscapes. These fully-supervised and real source-only supervised baselines indicate what the upper-bound of UDA generalization can realistically be. Without a theoretical foundation to derive a meaningful upper-bound, these experimental upper-bounds are the best alternative.

The results are shown in Tab. 4 and VFM-UDA++ and the most comparable upper-bounds are emphasized in gray for convenience. It can be seen that the alternative real source-only oracle achieves 83.0 mIoU and arguably is the most realistic upper bound for UDA, as its source data has a domain gap to the target unlike the fully-supervised oracle. This brings the gap of VFM-UDA++ even down to 0.8 mIoU. Regardless, if 83.0 mIoU or 85.0 mIoU (or one of the larger models) is a realistic upper bound for UDA, VFM-UDA++ with 82.2 mIoU is merely a few mIoU points separated from all upper bounds and demonstrates unprecedented strong generalization. This shows that providing

Method	#Parameters	GTAV → Cityscapes mIoU CS	All-synth → All-real mIoU CS
MIC B [20]	86M	75.9	73.7 ↓ -2.2
VFM-UDA S [12]	27M	71.3	74.8 ↑ +3.5
VFM-UDA B [12]	88M	77.1	79.1 ↑ +2.0
VFM-UDA L [12]	334M	78.4	80.8 ↑ +2.4
Source-only	334M	71.8	75.9
VFM-UDA++ S	27M	76.6	77.9 ↑ +1.3
VFM-UDA++ B	88M	79.1	80.6 ↑ +1.5
VFM-UDA++ L	334M	79.8	82.2 ↑ +2.4
Oracle	334M	85.0	85.0

Table 3. **All-synth to All-real benchmark.** VFM-UDA and VFM-UDA++ are able to scale with data obtaining improved generalization while MIC is not. The provided deltas are to the standard GTAV to Cityscapes results.

Architecture	Size	Setting	Source	Target	mIoU CS
VFM-UDA++	334M	UDA	GTAV	CS	79.8
VFM-UDA++	334M	UDA	GTAV,S,US	CS	81.5
VFM-UDA++	334M	UDA	All-synth	All-real	82.2
VLTseg [21]	304M	Source-only	GTAV	-	65.3
Rein [47]	350M	Source-only	GTAV	-	66.4
Rein [47]	350M	Source-only	GTA,S,US	-	78.4
VFM-UDA++ (oracle)	334M	Source-only	All-real w/o CS	-	83.0
VFM-UDA++ (oracle)	334M	fully-sup.	CS	-	85.0
ViT-Adapt [6] + M2F [7]	571M	fully-sup.	CS	-	85.8
MetaPrompt-SD [44]	912M	fully-sup.	CS	-	86.0

Table 4. **UDA versus supervised learning.** With more data, the generalization of VFM-UDA++ is very close to that of fully-supervised learning on all target labels.

VFM-UDA++ with more easy-to-generate synthetic source data and easy-to-obtain unlabeled real source data, is a very efficient and effective strategy to improve UDA and obtain generalization that is very close to fully-supervised learning without the need for target labels.

The strong generalization of VFM-UDA++ is further highlighted in Fig. 4, where we observe instances in which the model’s predictions surpass the accuracy of the ground-truth annotations, indicating that VFM-UDA++ effectively addresses labeling ambiguities and errors in the dataset.

4.4. Out-of-target generalization

In this experiment, we focus on the setting where the exact distribution of the target domain is unknown beforehand, *i.e.* the second goal of the *All-in* benchmark. This is relevant to many real-world UDA applications where a computer vision model can be deployed in an environment that cannot be fully anticipated beforehand. The results in Tab. 5 show the out-of-target mIoU of UDA methods on WildDash2 (WD2) when increasing data from GTAV, to GTAV and Cityscapes, and finally *All-synth* and *All-real*. For the out-of-target generalization we see a positive trend for all non-VFM and VFM UDA methods, in contrast to the in-target results in Tab. 3. The results in Tab. 3 and Tab. 5 show that the more diverse source and target data of *All-in* help UDA to generalize better to the broader out-of-target distribution of WildDash2, but not necessarily to the nar-

Method	Source	Target	mIoU WD2
Source-only	GTAV	-	40.6
MIC [20]	GTAV	CS	55.2 ↑ +4.6
MIC [20]	All-synth	All-real	60.1 ↑ +4.9
Source-only	GTAV	-	64.8
VFM-UDA [12]	GTAV	CS	65.5 ↑ +0.7
VFM-UDA [12]	All-synth	All-real	70.4 ↑ +4.9
Source-only	GTAV	-	65.5
VFM-UDA++	GTAV	CS	69.0 ↑ +3.5
VFM-UDA++	All-synth	All-real	71.3 ↑ +2.3

Table 5. **Out-of-target performance when scaling data.** All UDA methods scale with data for out-of-target generalization. The provided deltas are to the preceding row in the table.

rower in-target of Cityscapes. This significant increase in the out-of-target validation set contradicts the findings of [23], where they found that increasing unlabeled target data has diminishing returns. In the next section, we explore further the impact of data selection on UDA in-target and out-of-target generalization.

4.5. Data combination ablations

Scaling source and target data: In Tab. 6 we start with assessing the impact of individual synthetic datasets on the source-only generalization of VFM-based UDA. We can observe that each dataset’s benefit is insufficient to bridge the domain gap. However, when we combine them, their source-only generalization, thus not using any target images, reaches a level of 72.2 mIoU that is higher than some earlier UDA methods in Tab. 1. This is remarkable as it shows that with improved architectures, VFM-pretraining and only more source data, competitive levels of generalization can be obtained without using UDA.

Of course, the generalization can be improved further by UDA with target data. This is shown in the bottom half of Tab. 6. Here we show the different combinations of source and target data and their effect on UDA. The critical thing to note is that for in-target generalization on Cityscapes (CS), the generalization is best for *All-synth* to Cityscapes (79.3 mIoU) and reduces (73.4 mIoU) when more target data *All-real* is used. Even using less target data with GTAV to Cityscapes (77.1 mIoU) does better than more target data GTAV to *All-real* (73.4). This effect aligns with what we observed earlier for MIC in Tab. 3. So, the broader distribution in *All-real* consistently hurts generalization to the narrower target Cityscapes. But, we also observe that adding more diverse source data (*All-synth*) reduces this negative effect (78.6 mIoU). We also observe that adding more target data (*All-real*) consistently improves generalization to the broader out-of-target distribution of WildDash2.

From this, we can derive several important recommendations. Scaling labeled source data is a relatively safe approach to improving the generalization of UDA. When scal-

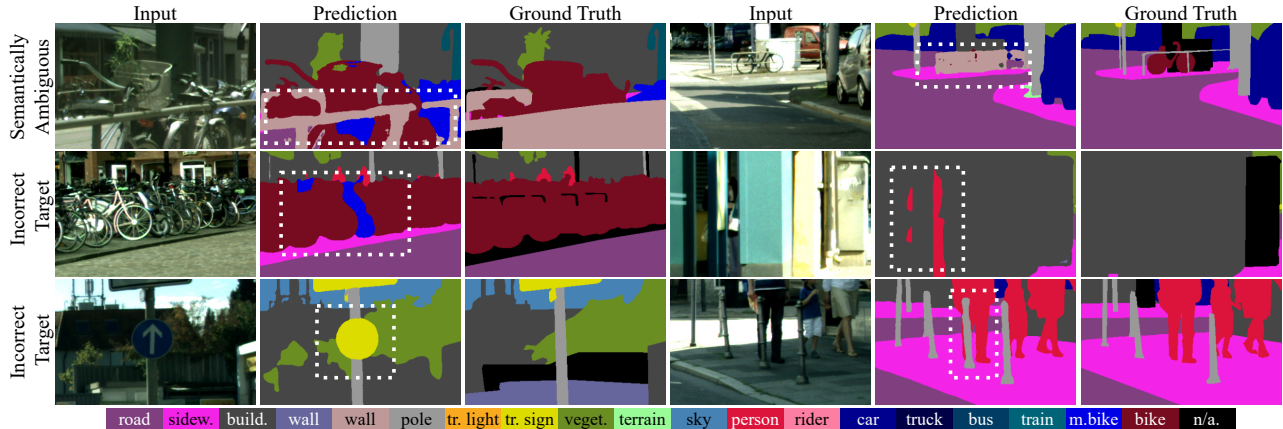


Figure 4. **Predictions by VFM-UDA++ can surpass ground truth accuracy.** Best viewed in high resolution. We observe that due to semantic ambiguity and manual labeling errors, the predictions of VFM-UDA++ can be more accurate than the ground truth. **Top left:** The model correctly predicts individual bars of the fence, while these are not labeled in the ground truth. **Top right:** The model predicts the entire fence, while now the individual bars are labeled. **Middle left:** The model correctly predicts a motorbike that is labeled as a bike. **Middle right:** The model correctly predicts a human that is not labeled. **Bottom left:** The model correctly predicts a traffic sign that is not labeled. **Bottom right:** The model correctly predicts a pole that is not labeled.

ing the target data, one needs to be more careful, as adding too much variety can also hurt in cases of generalization to a specific narrow target. It is highly advisable to scale source data when scaling target data, as it can compensate for the negative effect of too varied target data and help generalization.

Source	Target	mIoU CS	mIoU WD2
Synthia	-	46.4	33.1
Synscapes	-	59.7	45.5
GTAV	-	59.2	53.7
All-synth	-	72.2	58.8
GTAV	Cityscapes	77.1	61.3
All-synth	Cityscapes	79.3	61.8
GTAV	All-real	73.4	63.0
All-synth	All-real	78.6	67.1

Table 6. **Data combination ablations.** Showing that diversity in source data is beneficial, while diversity in target data can harm in-target generalization.

4.6. UDA architecture and training ablations

Ablation of multi-scale architecture: We start with choosing the VFM encoder and assess single-scale and multi-scale options. The benefit of a multi-scale VFM is that the multi-scale inductive bias can straightforwardly be used in UDA, while for single-scale VFMs additional components (e.g. ViT-Adapter [6]) are required. As shown in Tab. 7, the single-scale VFM DINOv2 [30] achieves the highest performance, with an in-target mIoU of 80.3% and an out-of-target mIoU of 68.6%, making it the preferred choice for VFM-UDA++. While the multi-scale VFMs are competitive and better than their non-VFM counterparts, their generalization is not on par with that of DINOv2.

While this might change in the future, for our research, it is essential to select the currently best available VFM and explore new levels of UDA generalization.

This brings us to the next ablation, where we assess options for introducing multi-scale inductive biases into UDA with a single-scale VFM. For this, we test several encoder and decoder configurations as shown in Tab. 8. We measure each setup’s effect on segmentation accuracy (mIoU) and computational efficiency (inference time). Starting with a baseline method VFM-UDA [12] with a ViT-B/14 [11] DINOv2 [30] pretrained encoder and a VFM-UDA decoder [12], we achieve an mIoU of 79.1%, which serves as the reference. Adding the ViT Adapter improves mIoU to 79.9% (+0.8 mIoU). However, adding two extra ViT Blocks without multi-scale capabilities—just to match the parameter count of the ViT Adapter—slightly decreases performance to 78.8% (-0.3 mIoU). This shows that the multi-scale capability and the inductive bias of the ViT-Adapter help in UDA.

For multi-scale decoder configurations, we evaluate *BasicPyramid*, DAFormer [18], HRDA [19], and Mask2Former [7] in conjunction with the ViT-Adapter. Among these, *BasicPyramid* achieves the most favorable inference time, showing that a more complicated decoder is unnecessary for UDA. Although HRDA, as also used by more recent MIC [20], and Mask2Former provide comparable performance (80.3% and 80.0%, respectively), they significantly increase computational demands, with inference time increasing by $5.09\times$ and $3.96\times$, respectively.

These findings suggest that *BasicPyramid* strikes the best balance between performance and efficiency when paired with the ViT-Adapter. It delivers strong segmentation

accuracy with minimal computational overhead compared to other decoder heads, making it the preferred architecture choice for VFM-UDA++.

Pre-training method	Multi-scale	In-target mIoU CS	Out-of-target mIoU WD2
SwinV2 [26]	✓	75.1	61.5
EVA-02 [13]	-	75.5	66.9
EVA-02-CLIP [40]	-	76.8	65.6
E-RADIO [34]	✓	78.9	68.2
DINOv2 [30]	-	79.1	68.0
DINOv2 [30] + ViT-Adapter [6]	✓	80.3	68.6

Table 7. **Ablation of different single-scale and multi-scale VFMs.** DINOv2 paired to a ViT-Adapter provides optimal generalization and up to +1.4 mIoU better than the best multi-scale VFM E-RADIO. Using the All-in benchmark with ViT-B/14 VFM-UDA++ model size for all metrics.

Encoder modification	Decoder	Multiscale encoder	Multi-scale decoder	#Param	Inference time	mIoU CS
-	VFM-UDA [12]	-	-	88M	1.00 ×	79.1
ViT-Adapter [6]	VFM-UDA [12]	✓	-	102M	1.81 ×	79.9
2 Extra ViT Blk.	VFM-UDA [12]	-	-	102M	1.05 ×	78.8
ViT-Adapter [6]	BasicPyramid	✓	✓	104M	1.80 ×	80.3
ViT-Adapter [6]	DAFormer [18]	✓	✓	104M	2.14 ×	79.7
ViT-Adapter [6]	HRDA [19]	✓	✓	109M	5.09 ×	80.3
ViT-Adapter [6]	Mask2Former [7]	✓	✓	120M	3.96 ×	80.0

Table 8. **Ablation of multi-scale encoder and decoder architectures with the All-in benchmark.** The results show the optimal mIoU vs. Inference time of using ViT-Adapter with our custom *BasicPyramid* decoder. The inference time is measured on an Nvidia H100 GPU with 16-bit mixed precision for ViT-B/14 model size.

Ablation of feature distance loss: Finally, shown in Tab. 9, we evaluated the effect of added feature distance (FD) losses on top of the VFM-UDA training strategies, comparing DaFormer’s feature distance loss to our modern VFM counterpart, which is not used before in the context of UDA. The VFM feature distance loss benefit is more pronounced in small-scale data settings where it adds +1.0 mIoU over VFM-UDA. When using a DINOv2-B feature extractor instead of a DINOv2-L, no benefit was observed. Although modest, it shows that a modern version of feature distance loss can help UDA generalization. In contrast, the DAFormer [18] feature distance loss used in SotA non-VFM methods decreases performance with -4.1 mIoU.

Source	Target	Baseline	w/ DaFormer’s FD loss [18]	w/ VFM FD loss	
GTAV	CS	78.1	74.0 ↓ -4.1	79.1 ↑ +1.0	mIoU CS
All-synth	All-real	80.3	79.9 ↓ -0.4	80.6 ↑ +0.3	mIoU CS

Table 9. **Relevance of feature distances losses in VFM-UDA++** We show that the VFM feature distance loss yields the best performance, while DaFormer’s feature distance loss decreases it slightly. Using the All-in benchmark with ViT-B/14 VFM-UDA++ architecture for all metrics.

5. Discussion

We identified two key limitations of VFM-UDA-its lack of multi-scale inductive bias and feature distance losses-and addressed them in VFM-UDA++ through multi-scale components and a modernized feature distance loss. While individual contributions may seem minor, their combined effect significantly enhances UDA generalization, bringing it close to supervised learning when sufficient data is available. Even small additions, such as the VFM feature distance loss, contribute to achieving this unprecedented level of generalization.

An important mIoU contribution in VFM-UDA++ comes from the ViT-Adapter paired to a custom multi-scale decoder, which introduces multi-scale inductive bias to the DINOv2 encoder, improving both in-target and out-of-target adaptation. Since strong multi-scale VFMs are currently unavailable, ViT adapters and custom decoders remain necessary. Although E-RADIO is a competitive alternative, DINOv2 proves superior in generalization. As native multi-scale VFMs improve, the need for our approach may diminish, but the importance of multi-scale inductive bias in VFM UDA generalization remains a key takeaway.

6. Conclusions

This work addresses three fundamental research questions: (i) How can architectural enhancements further improve VFM-UDA performance? (ii) To what extent can scaling data enhance VFM-UDA generalization? (iii) To what extent do these improvements reduce the generalization gap between UDA and fully-supervised learning? In response, we developed VFM-UDA++, which achieves state-of-the-art generalization results across various benchmarks. The primary contribution of this study is demonstrating that through targeted architectural improvements and straightforward scaling of synthetic and unlabeled real data, VFM-UDA++ attains performance remarkably close to fully-supervised learning. Specifically, the remaining performance gap to an upper-bound generalization is reduced to just a few mIoU points, representing a significant milestone in UDA research.

Importantly, our findings suggest that fundamentally novel UDA techniques are not strictly necessary for further enhancing UDA generalization. Instead, substantial gains can be achieved by effectively upgrading established UDA principles with modern vision model architectures and pre-training strategies. Nonetheless, addressing existing limitations, particularly training instability arising from error reinforcement, remains crucial before large-scale usage of UDA becomes feasible. With the robust generalization results provided by VFM-UDA++, we encourage future research in UDA and hope to contribute to its applicability.

VFM-UDA++: Improving Network Architectures and Data Strategies for Unsupervised Domain Adaptive Semantic Segmentation

Supplementary Material

Overview

The additional experiments that we provide are:

- Sec. 7: Per-class performance analysis
- Sec. 8: Extended results for benchmarks
- Sec. 9: VFM-UDA training ablation
- Sec. 10: Inference time analysis
- Sec. 11: All-synth dataset statistics
- Sec. 12: Benchmark (in)stability analysis

7. Per-class performance analysis on the GTA5-to-Cityscapes benchmark

The results in Tab. 10 provide a detailed per-class performance analysis of VFM-UDA++ compared to other state-of-the-art UDA methods on the GTA5-to-Cityscapes benchmark. VFM-UDA++ consistently outperforms other approaches, with significant gains in underrepresented or challenging classes such as rider (+10.0% over MIC), train (+8.4%), and motorbike (+8.0%). These improvements highlight the effectiveness of VFM-UDA++ in addressing class imbalances and rare categories, a persistent challenge in UDA. However, MIC achieves better results in the 'traffic sign', 'sky' and 'vegetation' categories, VFM-UDA++ excels in all other categories, making it the overall preferred choice for urban segmentation.

8. Extended results for benchmarks

Tab. 10 and Tab. 11 provide the results on the GTAV to Cityscape and All-in benchmarks including all source-only and oracle results per method.

9. Ablation of training strategies

In this experiment, we investigate the effect of various existing training strategies on the UDA performance of VFM-UDA++'s architecture. We use VFM-UDA's training strate-

gies [12] as a starting point, achieving a baseline performance of 80.3% mIoU on the All-In benchmark.

To assess the importance of individual training strategies, we evaluated the impact of their removal on UDA performance. Removing the learning rate multiplier between encoder and decoder layers and Domain Adaptation via Cross-domain Mixed Sampling (DACS) [42], which facilitates cross-domain mixing, resulted in the most significant performance drops (reductions of 10.0% and 7.4% mIoU, respectively). In contrast, excluding other components, such as the Exponential Moving Average (EMA) model for stabilizing pseudo-label generation, masking loss [20], and pseudo-label weighting [15, 29], led to smaller reductions in mIoU. Rare class sampling [18] did not seem to increase or decrease mIoU, but for cases of severe source class label imbalances, it is advisable to keep it included in UDA.

10. Inference time analysis

Tab. 14 compares the inference times of various methods and architectures under different configurations, using MIC as the baseline for comparison. Notably, we significantly improved MIC's performance, compared to the original implementation, by incorporating Flash Attention [10] and batched sliding window inference (instead of a Python for-loop). These improvements result in an inference time reduction from 239.0 ms to 85.8 ms, making our MIC [20] reimplementation a strong baseline for evaluating segmentation performance versus computational cost. VFM-UDA++ demonstrates a favorable balance between accuracy and computational efficiency. For instance, VFM-UDA++ with a ViT-B/14 backbone achieves a competitive 79.1% mIoU while maintaining a $2.5\times$ speedup compared to MIC. Interestingly, the ViT-S/14 backbone offers 44.6 FPS with only a minor performance drop, making it suitable for real-time applications. These findings suggest that VFM-UDA++ can be adapted for scenarios requiring high performance

Method	Road	S.walk	Build.	Wall	Fence	Pole	Tr.Light	Sign	Veget.	Terrain	Sky	Person	Rider	Car	Truck	Bus	Train	M.bike	Bike	mIoU
DAFormer [18]	95.7	70.2	89.4	53.5	48.1	49.6	55.8	59.4	89.9	47.9	92.5	72.2	44.7	92.3	74.5	78.2	65.1	55.9	61.8	68.3
HRDA [19]	96.4	74.4	91.0	61.6	51.5	57.1	63.9	69.3	91.3	48.4	94.2	79.0	52.9	93.9	84.1	85.7	75.9	63.9	67.5	73.8
MIC [20]	97.4	80.1	91.7	61.2	56.9	59.7	66.0	71.3	91.7	51.4	94.3	79.8	56.1	94.6	85.4	90.3	80.4	64.5	68.5	75.9
VFM-UDA [12]	97.5	80.4	92.0	61.5	66.0	60.7	71.1	71.8	90.4	46.6	90.8	81.7	57.4	95.0	87.6	92.9	85.4	70.7	65.4	77.1
VFM-UDA++ (ViT-B/14)	98.0	82.2	92.1	63.3	66.5	64.6	74.0	69.2	89.9	48.0	89.3	84.0	66.1	95.8	91.4	94.7	88.8	72.5	71.7	79.1
VFM-UDA++ (ViT-L/14)	97.1	78.7	92.3	66.9	62.0	66.7	74.1	69.4	91.0	53.0	92.0	84.4	68.2	95.6	91.9	95.3	91.2	74.4	73.0	79.8

Table 10. **Per-class performance analysis on the GTA5-to-Cityscapes benchmark.** VFM-UDA++ outperforms state-of-the-art methods on challenging classes such as rider, train, and motorbike, showcasing its ability to address class imbalances effectively.

Method	Backbone	Pre-training	# Parameters	In-target mIoU			Out-of-target mIoU		
				Source-only	UDA	Oracle	Source-only	UDA	Oracle
DaFormer [18]	MiT-B5	ImageNet-1K [37]	85M	47.1	68.3	76.6	41.9	50.1	66.8
SePiCo [49]	MiT-B5	ImageNet-1K [37]	85M	46.5	70.3	78.3	37.7	47.5	64.8
HRDA [19]	MiT-B5 [50]	ImageNet-1K [37]	86M	47.3	73.8	80.8	40.6	50.8	66.9
MIC [20]	MiT-B5 [50]	ImageNet-1K [37]	86M	47.3	75.9	80.8	40.6	55.2	66.9
VFM-UDA [12]	ViT-S/14	DINOv2 [30]	23M	62.0	71.3	80.9	54.3	55.6	71.4
VFM-UDA [12]	ViT-B/14	DINOv2 [30]	88M	62.9	77.1	82.4	60.4	60.8	74.8
VFM-UDA [12]	ViT-L/14	DINOv2 [30]	308M	68.7	78.4	83.4	64.8	65.5	76.3
VFM-UDA++	ViT-S/14	DINOv2 [30]	27M	62.2	76.6	82.7	55.8	60.5	73.3
VFM-UDA++	ViT-B/14	DINOv2 [30]	104M	68.5	79.1	84.4	62.6	65.2	76.4
VFM-UDA++	ViT-L/14	DINOv2 [30]	334M	71.8	79.8	85.0	65.5	69.0	77.7

Table 11. **Performance comparison on the GTA5-to-Cityscapes benchmark.** VFM-UDA++ consistently outperforms previous methods across multiple model scales on the in-target metric, significantly improving the out-of-target metric.

Method	Backbone	Pre-training	# Parameters	In-target mIoU			Out-of-target mIoU		
				Source-only	UDA	Oracle	Source-only	UDA	Oracle
MIC [20]	MiT-B5 [50]	ImageNet-1K [37]	86M	64.3	73.7	80.8	46.6	60.1	66.9
VFM-UDA [12]	ViT-S/14	DINOv2 [30]	23M	68.1	74.8	80.9	58.5	63.9	71.5
VFM-UDA [12]	ViT-B/14	DINOv2 [30]	88M	72.5	79.1	82.4	59.6	68.0	70.6
VFM-UDA [12]	ViT-L/14	DINOv2 [30]	308M	75.4	80.8	83.4	62.9	70.4	73.2
VFM-UDA++	ViT-S/14	DINOv2 [30]	27M	69.4	77.9	82.7	59.1	67.8	73.3
VFM-UDA++	ViT-B/14	DINOv2 [30]	104M	73.8	80.6	84.4	63.7	69.5	76.4
VFM-UDA++	ViT-L/14	DINOv2 [30]	334M	75.9	82.2	85.0	67.2	71.3	77.7

Table 12. **Performance comparison on the All-in benchmark.** The results show that ViT-L/14 based model under VFM-UDA++ achieve close performance to the oracle. Notably, VFM-UDA++ outperforms VFM-UDA [12] across all model sizes and all metrics, with more pronounced gains observed as model capacity increases.

EMA model	Pseudo weight	LR multiplier	DACS [42]	Rare Class Sampling [18]	Masked Image Consistency [20]	mIoU CS
✓	✓	✓	✓	✓	✓	80.3
-	✓	✓	✓	✓	✓	79.3 ↓ -1.0
✓	-	✓	✓	✓	✓	79.3 ↓ -1.0
✓	✓	-	✓	✓	✓	70.3 ↓ -10.0
✓	✓	✓	-	✓	✓	72.9 ↓ -7.4
✓	✓	✓	✓	-	✓	80.3 ≈
✓	✓	✓	✓	✓	-	78.4 ↓ -1.9

Table 13. **Ablation of VFM-UDA training strategies with the new All-in benchmark.** The results show that the learning rate multiplier and DACS are the most critical UDA strategies for VFM-UDA++. Using ViT-B/14 model size for all metrics.

or computational efficiency without significant trade-offs in segmentation accuracy.

11. All-synth dataset statistics

Fig. 5 provides a breakdown of class distributions across the GTA5 and All-synth datasets. While GTA5 suffers from severe class imbalances (e.g., bicycles appear in only 440 images), the All-synth dataset significantly reduces these disparities, with all classes receiving more balanced representation. In practical UDA applications, such severe class

Method	Image size (px)	mIoU	Time (ms)	Speedup
MIC (MiT-B5)	1024×1024	75.9	85.8	1.0×
DaFormer (MiT-B5)	512×512	68.3	33.3	2.6×
HRDA (MiT-B5)	1024×1024	73.8	85.8	1.0×
MIC (original impl.) (MiT-B5)	1024×1024	75.9	239.0	0.4×
MIC (MiT-B5)	1024×1024	75.9	85.8	1.0×
VFM-UDA (ViT-S/14)	1024×1024	71.3	8.9	9.6×
VFM-UDA (ViT-B/14)	1024×1024	77.1	15.8	5.4×
VFM-UDA (ViT-L/14)	1024×1024	78.3	34.7	2.5×
VFM-UDA++ (ViT-S/14)	1024×1024	76.6	22.4	3.8×
VFM-UDA++ (ViT-B/14)	1024×1024	79.1	33.4	2.5×
VFM-UDA++ (ViT-L/14)	1024×1024	79.8	56.0	1.5×

Table 14. **Efficiency and performance trade-off for UDA methods.** The VFM-UDA++ ViT-B/14 achieves a strong 79.1% mIoU with a 2.5× speedup compared to MIC, making it suitable for high-performance setups. The ViT-S/14 variant offers real-time capabilities with minimal performance loss. The inference time is measured on an Nvidia H100 GPU with 16-bit mixed precision.

imbalances would not be intentionally introduced, as they undermine performance and generalization. This highlights the importance of considering more balanced datasets, like All-in, in UDA research to better reflect real-world scenar-

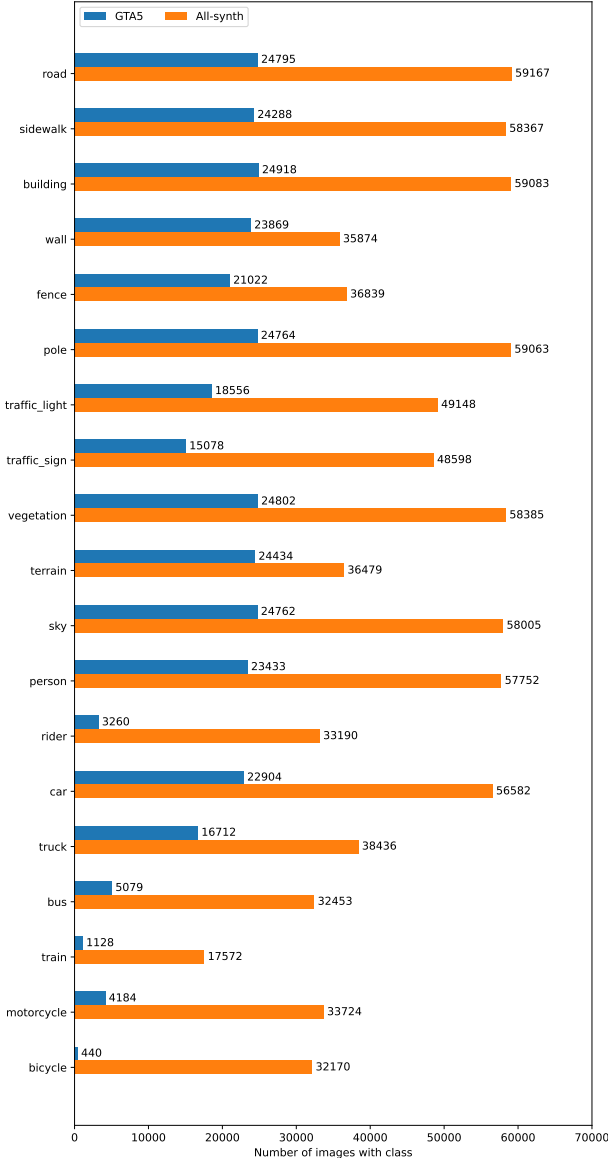


Figure 5. **Class distribution comparison between GTA5 and All-synth datasets.** The All-synth dataset improves the class imbalance, present in GTA5. This diversity contributes to improved stability in UDA benchmarking.

ios and improve evaluation reliability. This diversity explains the improved stability and performance observed in the All-in benchmark compared to traditional setups like GTA5-to-Cityscapes, as discussed in Sec. 12.

12. Benchmark (in)stability analysis

In this experiment, we assess the stability of UDA benchmark results by examining performance variation across different random seeds. Tab. 15 compares the standard de-

Method	Statistic	GTAV to City. mIoU CS	All-in mIoU CS
MIC [20]	best seed	76.2	73.4
MIC [20]	worst seed	70.3	73.9
MIC [20]	average	74.8	73.7
MIC [20]	std dev	1.9	0.2
VFM-UDA [12]	best seed	77.1	79.3
VFM-UDA [12]	worst seed	75.1	78.2
VFM-UDA [12]	average	76.1	78.8
VFM-UDA [12]	standard deviation	0.6	0.4
VFM-UDA++	best seed	79.5	81.0
VFM-UDA++	worst seed	78.8	80.2
VFM-UDA++	average	79.1	80.6
VFM-UDA++	std dev	0.3	0.3

Table 15. **Instability in UDA over six runs.** By using more data in pretraining (VFM-UDA++) or during UDA (All-in benchmark), stability of UDA can be improved significantly.

viation in mIoU over six random seeds for MIC [20] and VFM-UDA++ on both the GTAV-to-Cityscapes and the All-in benchmarks. The standard deviation in the GTAV-to-Cityscapes setup is notably higher, specifically for the non-VFM method, due to GTAV’s limited diversity and severe label imbalance. Although techniques like *rare class sampling* [18] are used in MIC [20], to mitigate class label collapse [18] where certain classes drop to zero IoU and fail to recover during training, class label collapse cannot be fully prevented by rare class sampling and thus results in high variance. This data instability underscores the limitations of GTAV as a source domain for robust UDA evaluation and makes fair comparisons hard, highlighting the need for our All-in benchmark. On the All-in benchmark, both the non-VFM and the VFM-UDA++ approaches demonstrate proper stability over random seeds. It is also noticeable that VFM-UDA++ does not suffer from instability on the GTAV-to-Cityscapes benchmark, which is a benefit of its VFM’s stronger pretraining.

References

- [1] Abien Fred Agarap. Deep learning using rectified linear units (ReLU). *CoRR*, abs/1803.08375, 2018. 3
- [2] Nikita Araslanov and Stefan Roth. Self-supervised Augmentation Consistency for Adapting Semantic Segmentation. In *CVPR*, 2021. 2, 3
- [3] Mu Chen, Zhedong Zheng, Yi Yang, and Tat-Seng Chua. Pipa: Pixel- and patch-wise self-supervised learning for domain adaptive semantic segmentation. In *ACM Multimedia*. ACM, 2023. 2, 5
- [4] Mu Chen, Zhedong Zheng, and Yi Yang. Transferring to real-world layouts: A depth-aware framework for scene adaptation. In *ACM Multimedia*, 2024. 2, 5
- [5] Ting Chen, Simon Kornblith, Mohammad Norouzi, and Geoffrey E. Hinton. A Simple Framework for Contrastive Learning of Visual Representations. In *ICML*, 2020. 3
- [6] Zhe Chen, Yuchen Duan, Wenhai Wang, Junjun He, Tong

- Lu, Jifeng Dai, and Yu Qiao. Vision transformer adapter for dense predictions. In *ICLR*, 2023. 3, 4, 6, 7, 8
- [7] Bowen Cheng, Ishan Misra, Alexander G. Schwing, Alexander Kirillov, and Rohit Girdhar. Masked-attention mask transformer for universal image segmentation. In *CVPR*, 2022. 3, 6, 7, 8
- [8] Marius Cordts, Mohamed Omran, Sebastian Ramos, Timo Rehfeld, Markus Enzweiler, Rodrigo Benenson, Uwe Franke, Stefan Roth, and Bernt Schiele. The Cityscapes Dataset for Semantic Urban Scene Understanding. In *CVPR*, 2016. 5
- [9] Dengxin Dai and Luc Van Gool. Dark model adaptation: Semantic image segmentation from daytime to nighttime. In *ITSC*, 2018. 5
- [10] Tri Dao, Daniel Y. Fu, Stefano Ermon, Atri Rudra, and Christopher Ré. FlashAttention: Fast and memory-efficient exact attention with IO-awareness. In *NeurIPS*, 2022. 1
- [11] Alexey Dosovitskiy, Lucas Beyer, Alexander Kolesnikov, Dirk Weissenborn, Xiaohua Zhai, Thomas Unterthiner, Mostafa Dehghani, Matthias Minderer, Georg Heigold, Sylvain Gelly, Jakob Uszkoreit, and Neil Houlsby. An Image is Worth 16x16 Words: Transformers for Image Recognition at Scale. In *ICLR*, 2021. 2, 3, 7
- [12] Englert, Brunó B., Piva, Fabrizio J., Kerssies, Tommie, de Geus, Daan, and Dubbelman, Gijs. Exploring the benefits of vision foundation models for unsupervised domain adaptation. In *CVPR Workshops*, 2024. 1, 2, 3, 5, 6, 7, 8
- [13] Yuxin Fang, Quan Sun, Xinggang Wang, Tiejun Huang, Xinlong Wang, and Yue Cao. EVA-02: A Visual Representation for Neon Genesis. *arXiv preprint arXiv:2303.11331*, 2023. 1, 8
- [14] Yuxin Fang, Wen Wang, Binhui Xie, Quan Sun, Ledell Wu, Xinggang Wang, Tiejun Huang, Xinlong Wang, and Yue Cao. EVA: exploring the limits of masked visual representation learning at scale. In *CVPR*, pages 19358–19369. IEEE, 2023. 1
- [15] Geoffrey French, Timo Aila, Samuli Laine, Michal Mackiewicz, and Graham D. Finlayson. Consistency regularization and cutmix for semi-supervised semantic segmentation. *CoRR*, abs/1906.01916, 2019. 3, 1
- [16] Kaiming He, Xinlei Chen, Saining Xie, Yanghao Li, Piotr Dollár, and Ross B. Girshick. Masked Autoencoders Are Scalable Vision Learners. In *CVPR*, 2022. 3
- [17] Judy Hoffman, Dequan Wang, Fisher Yu, and Trevor Darrell. Fcns in the wild: Pixel-level adversarial and constraint-based adaptation. *CoRR*, abs/1612.02649, 2016. 1
- [18] Lukas Hoyer, Dengxin Dai, and Luc Gool. DAFormer: Improving network architectures and training strategies for domain-adaptive semantic segmentation. In *CVPR*, 2022. 1, 2, 3, 4, 5, 7, 8
- [19] Lukas Hoyer, Dengxin Dai, and Luc Gool. HRDA: Context-aware high-resolution domain-adaptive semantic segmentation. In *ECCV*, 2022. 2, 3, 5, 7, 8, 1
- [20] Lukas Hoyer, Dengxin Dai, Haoran Wang, and Luc Van Gool. MIC: Masked Image Consistency for Context-Enhanced Domain Adaptation. In *CVPR*, 2023. 2, 3, 4, 5, 6, 7, 1
- [21] Christoph Hümmer, Manuel Schwonberg, Liangwei Zhou, Hu Cao, Alois Knoll, and Hanno Gottschalk. Strong but simple: A baseline for domain generalized dense perception by clip-based transfer learning. In *Asian Computer Vision Conference*, 2024. 6
- [22] Sergey Ioffe and Christian Szegedy. Batch normalization: Accelerating deep network training by reducing internal covariate shift. In *ICML*, pages 448–456, 2015. 3
- [23] Tarun Kalluri, Sreyas Ravichandran, and Manmohan Chandraker. Uda-bench: Revisiting common assumptions in unsupervised domain adaptation using a standardized framework. *ECCV*, 2024. 6
- [24] Samuli Laine and Timo Aila. Temporal ensembling for semi-supervised learning. In *ICLR*, 2017. 2, 3
- [25] Yann LeCun, Yoshua Bengio, and Geoffrey Hinton. Deep learning. *Nature*, 521(7553):436, 2015. 3
- [26] Ze Liu, Han Hu, Yutong Lin, Zhuliang Yao, Zhenda Xie, Yixuan Wei, Jia Ning, Yue Cao, Zheng Zhang, Li Dong, Furu Wei, and Baining Guo. Swin transformer v2: Scaling up capacity and resolution. In *International Conference on Computer Vision and Pattern Recognition (CVPR)*, 2022. 8
- [27] Ilya Loshchilov and Frank Hutter. Decoupled weight decay regularization. In *ICLR*, 2019. 4
- [28] Gerhard Neuhold, Tobias Ollmann, Samuel Rota Bulò, and Peter Kotschieder. The Mapillary Vistas Dataset for Semantic Understanding of Street Scenes. In *ICCV*, 2017. 5
- [29] Viktor Olsson, Wilhelm Tranheden, Juliano Pinto, and Lennart Svensson. Classmix: Segmentation-based data augmentation for semi-supervised learning. In *WACV*, pages 1369–1378, 2021. 3, 1
- [30] Maxime Oquab, Timothée Darcet, Théo Moutakanni, Huy Vo, Marc Szafraniec, Vasil Khalidov, Pierre Fernandez, Daniel Haziza, Francisco Massa, Alaaeldin El-Nouby, Mahmoud Assran, Nicolas Ballas, Wojciech Galuba, Russell Howes, Po-Yao Huang, Shang-Wen Li, Ishan Misra, Michael G. Rabbat, Vasu Sharma, Gabriel Synnaeve, Hu Xu, Hervé Jégou, Julien Mairal, Patrick Labatut, Armand Joulin, and Piotr Bojanowski. DINOv2: Learning Robust Visual Features without Supervision. *TMLR*, 2024. 1, 2, 3, 7, 8
- [31] Duo Peng, Ping Hu, Qihong Ke, and Jun Liu. Diffusion-based Image Translation with Label Guidance for Domain Adaptive Semantic Segmentation. In *2023 IEEE/CVF International Conference on Computer Vision (ICCV)*, pages 808–820, Los Alamitos, CA, USA, 2023. IEEE Computer Society. 2, 5
- [32] Fabrizio J. Piva, Daan de Geus, and Gijs Dubbelman. Empirical generalization study: Unsupervised domain adaptation vs. domain generalization methods for semantic segmentation in the wild. In *Proceedings of the IEEE/CVF Winter Conference on Applications of Computer Vision (WACV)*, pages 499–508, 2023. 4
- [33] Alec Radford, Jong Wook Kim, Chris Hallacy, Aditya Ramesh, Gabriel Goh, Sandhini Agarwal, Girish Sastry, Amanda Askell, Pamela Mishkin, Jack Clark, Gretchen Krueger, and Ilya Sutskever. Learning Transferable Visual Models From Natural Language Supervision. In *ICML*, 2021. 3

- [34] Mike Ranzinger, Greg Heinrich, Jan Kautz, and Pavlo Molchanov. AM-RADIO: Agglomerative vision foundation model reduce all domains into one. In *CVPR*, pages 12490–12500, 2024. 3, 8
- [35] Stephan R. Richter, Vibhav Vineet, Stefan Roth, and Vladlen Koltun. Playing for Data: Ground Truth from Computer Games. In *ECCV*, 2016. 5
- [36] German Ros, Laura Sellart, Joanna Materzynska, David Vazquez, and Antonio M. Lopez. The SYNTHIA Dataset: A Large Collection of Synthetic Images for Semantic Segmentation of Urban Scenes. In *CVPR*, 2016. 5
- [37] Olga Russakovsky, Jia Deng, Hao Su, Jonathan Krause, Sanjeev Satheesh, Sean Ma, Zhiheng Huang, Andrej Karpathy, Aditya Khosla, Michael S. Bernstein, Alexander C. Berg, and Li Fei-Fei. ImageNet Large Scale Visual Recognition Challenge. *IJCV*, 115(3):211 – 252, 2015. 2
- [38] Christos Sakaridis, Dengxin Dai, and Luc Van Gool. ACDC: the adverse conditions dataset with correspondences for semantic driving scene understanding. In *ICCV*, pages 10745–10755. IEEE, 2021. 5
- [39] Fengyi Shen, Akhil Gurram, Ziyuan Liu, He Wang, and Alois Knoll. Diga: Distil to generalize and then adapt for domain adaptive semantic segmentation. In *Proceedings of the IEEE/CVF Conference on Computer Vision and Pattern Recognition*, pages 15866–15877, 2023. 2, 5
- [40] Quan Sun, Yuxin Fang, Ledell Wu, Xinlong Wang, and Yue Cao. EVA-CLIP: Improved Training Techniques for CLIP at Scale. *arXiv preprint arXiv:2303.15389*, 2023. 8
- [41] Antti Tarvainen and Harri Valpola. Mean teachers are better role models: Weight-averaged consistency targets improve semi-supervised deep learning results. In *NeurIPS*, pages 1195–1204., 2017. 3
- [42] Wilhelm Tranheden, Viktor Olsson, Juliano Pinto, and Lennart Svensson. DACS: Domain Adaptation via Crossdomain Mixed Sampling. In *WACV*, pages 1379–1389., 2021. 2, 4, 1
- [43] Midhun Vayyat, Jaswin Kasi, Anuraag Bhattacharya, Shuaib Ahmed, and Rahul Tallamraju. CLUDA: Contrastive Learning in Unsupervised Domain Adaptation for Semantic Segmentation. *arXiv preprint arXiv:2208.14227*, 2022. 2, 3
- [44] Qiang Wan, Ming Nie, Zilong Huang, Bingyi Kang, Jiashi Feng, and Li Zhang. Harnessing diffusion models for visual perception with meta prompts. *arXiv preprint arXiv:2312.14733*, 2023. 6
- [45] Kaihong Wang, Donghyun Kim, Rogério Feris, and Margrit Betke. Cdac: Cross-domain attention consistency in transformer for domain adaptive semantic segmentation. pages 11485–11495, 2023. 2, 5
- [46] Qin Wang, Dengxin Dai, Lukas Hoyer, Olga Fink, and Luc Gool. Domain adaptive semantic segmentation with self-supervised depth estimation. In *ICCV*, pages 85158525., 2021. 2, 5
- [47] Zhixiang Wei, Lin Chen, Yi Jin, Xiaoxiao Ma, Tianle Liu, Pengyang Ling, Ben Wang, Huaian Chen, and Jinjin Zheng. Stronger, Fewer, & Superior: Harnessing Vision Foundation Models for Domain Generalized Semantic Segmentation. In *CVPR*, 2024. 2, 5, 6
- [48] Magnus Wrenninge and Jonas Unger. Synscapes: A photorealistic synthetic dataset for street scene parsing. *CoRR*, abs/1810.08705, 2018. 5
- [49] Binhui Xie, Shuang Li, Mingjia Li, Chi Harold Liu, Gao Huang, and Guoren Wang. SePiCo: Semantic-Guided Pixel Contrast for Domain Adaptive Semantic Segmentation. *IEEE TPAMI*, 45(07):9004–9021, 2023. 2, 3, 5
- [50] Enze Xie, Wenhai Wang, Zhiding Yu, Anima Anandkumar, José M. Álvarez, and Ping Luo. SegFormer: Simple and Efficient Design for Semantic Segmentation with Transformers. In *NeurIPS*, 2021. 2
- [51] Zhenda Xie, Zheng Zhang, Yue Cao, Yutong Lin, Jianmin Bao, Zhuliang Yao, Qi Dai, and Han Hu. SimMIM: a Simple Framework for Masked Image Modeling. In *CVPR*, 2022. 3
- [52] Fisher Yu, Haofeng Chen, Xin Wang, Wenqi Xian, Yingying Chen, Fangchen Liu, Vashisht Madhavan, and Trevor Darrell. BDD100K: A diverse driving dataset for heterogeneous multitask learning. In *CVPR*, 2020. 5
- [53] Pan Zhang, Bo Zhang, Ting Zhang, Dong Chen, Yong Wang, and Fang Wen. Prototypical pseudo label denoising and target structure learning for domain adaptive semantic segmentation. In *CVPR*, pages 12414–12424., 2021. 2, 5